European Journal of Pharmaceutics and Biopharmaceutics 138 (2019) 99–110

Contents lists available at ScienceDirect

European Journal of Pharmaceutics and Biopharmaceutics

journal homepage: www.elsevier.com/locate/ejpb

Research paper

3D printed, controlled release, tritherapeutic tablet matrix for advanced anti-HIV-1 drug delivery

Margaret Siyawamwaya, Lisa C. du Toit, Pradeep Kumar, Yahya E. Choonara, Pierre P.P.D. Kondiah, Viness Pillay*

Wits Advanced Drug Delivery Platform Research Unit, Department of Pharmacy and Pharmacology, School of Therapeutic Sciences, Faculty of Health Sciences, University of the Witwatersrand, Johannesburg, 7 York Road, Parktown 2193, South Africa

ARTICLE INFO

Keywords:
3D printing
Fixed dose combination
Anti-HIV-1 drugs
Efavirenz
Tenofovir disoproxil fumarate
Emtricitabine

ABSTRACT

Purpose: A 3D-Bioplotter® was employed to 3D print (3DP) a humic acid-polyquaternium 10 (HA-PQ10) controlled release fixed dose combination (FDC) tablet comprising of the anti-HIV-1 drugs, efavirenz (EFV), tenofovir disoproxil fumarate (TDF) and emtricitabine (FTC).
Methods: Chemical interactions, surface morphology and mechanical strength of the FDC were ascertained. *In vitro* drug release studies were conducted in biorelevant media followed by *in vivo* study in the large white pigs, in comparison with a market formulation, Atripla®. *In vitro-in vivo* correlation of results was undertaken.
Results: EFV, TDF and FTC were successfully entrapped in the 24-layered rectangular prism-shaped 3DP FDC with a loading of ~12.5 mg/6.3 mg/4 mg of EFV/TDF/FTC respectively per printed layer. Hydrogen bonding between the EFV/TDF/FTC and HA-PQ10 was detected which was indicative of possible drug solubility enhancement. The overall surface of the tablet exhibited a fibrilla structure and the 90° inner pattern was determined to be optimal for 3DP of the FDC. *In vitro and in vivo* drug release profiles from the 3DP FDC demonstrated that intestinal-targeted and controlled drug release was achieved.
Conclusion: A 3DP FDC was successfully manufactured with the aid of a 3D-Bioplotter in a single step process. The versatile HA-PQ10 entrapped all drugs and achieved an enhanced relative bioavailability of EFV, TDF, and FTC compared to the market formulation for potentially enhanced HIV treatment.

1. Introduction

3D Printing (3DP) constitutes an innovative rapid prototyping technique for tablet manufacture which is of growing interest in pharmaceutical research [1]. 3DP is revolutionizing the field of drug delivery by enabling the synthesis of customized and digitally-controlled tablets in a layer-by-layer manner thus allowing for a convenient no-contact approach to imparting diverse modifications to the dosage form design. This technique is highly attractive allowing for precise and enhanced drug-loading capacity [2]. The process of 3DP constitutes pharmaceutical material deposited on a build platform that gradually develops into a 3D object (or solid dosage form i.e. a tablet) using precise computer-aided geometry. The 3D-printing device is able to print in XYZ co-ordinates and it also utilizes compressed air to regulate the flow of the sludge [3]. 3DP contributes to more end-stage customization of solid dosage forms such as tablets [4]. One of the 3D-printing variations is Fused Deposition Modeling (FDM) which has been widely used with success in manufacturing solid dosage forms [1]. However, one of the drawbacks of using the technique is that thermolabile drugs or polymers cannot be processed; therefore developing pharma inks which are functional at ambient temperatures is a necessity. In order to advance the research currently in the pharmaceutical field, this study focused on the design, characterization and evaluation of a novel 3D-printed Fixed-Dose Combination (FDC) tablet comprising a humic acid-polyquaternium 10 complex (HA-PQ10) as the 'pharma-ink' to achieve controlled release of three anti-HIV drugs, namely efavirenz (EFV), tenofovir disoproxil fumarate (TDF) and emtricitabine (FTC) as the model HIV treatment regimen. The previously reported unique 'printable' properties of HA and PQ10 inspired the application of this complex for designing the 3DP FDC tablet in this study [5–7]. It has been demonstrated that the HA-PQ10 polyelectrolyte complex was a biocompatible complex capable of significantly enhancing the solubility and permeability of drugs [6,7]. Furthermore, the matrix system can load both hydrophilic and lipophilic drugs due to the amphiphilic nature of HA. Employing an ambient temperature setting for 3DP was imperative since HA and PQ10 are not

* Corresponding author.
E-mail address: viness.pillay@wits.ac.za (V. Pillay).

https://doi.org/10.1016/j.ejpb.2018.04.007
Received 18 January 2018; Received in revised form 9 April 2018; Accepted 11 April 2018
Available online 12 April 2018
0939-6411/

thermoplastic.

A study undertaken by Katstra and co-workers [8] demonstrated that oral tablets can be manufactured by 3DP with drug release patterns comparable to routine compressed formulations. However, 3DP provides additional benefits for tablet design through the use of advanced computer aided design (CAD). A variety of tablet structural designs that are easily modifiable digitally can be printed [9,10]. This flexibility of 3DP renders it suitable for the design of innovative personalized medicines for small-scale tablet manufacture. This approach would also be beneficial in the use of drugs with limited shelf-life. The process is not only making headway for novel drug delivery technologies but also offers a potentially cost-effective manufacturing method for tablets [11].

Interestingly, as previously demonstrated, HA and PQ10 are polyelectrolytes that can partially self-assemble when processed as a sludge [6]. This study thus aimed to utilize a single-step 3DP as an alternative manufacturing technique to formulate a controlled release prototype FDC tablet using pre-blended and partially self-assembled HA and PQ10 as the polyelectrolyte framework to control the release of EFV, TDF and FTC as the recommended first-line treatment drugs for HIV-1 [12]. These drugs are also listed within different classes of the Biopharmaceutics Classification System (BCS) (EFV = class II, TDF = class III and FTC = class I) and thus useful to test the feasibility of the 3DP tablet to control the release of hydrophilic and lipophilic drug molecules. In addition, tableting by compaction of dry powder blends produces tablets with heterogeneous swelling rates with less control in drug release patterns [13]. The extrusion-based deposition model used in 3DP may result in significant microstructural modification of drug diffusivity through the 3DP tablet matrix to influence the drug release kinetics [14]. A previous study by Khaled and co-workers [15] showed that 3DP can successfully synthesize sustained release tablets using a viscous paste as the 'printing ink'. To the best of our knowledge, there is no 3DP FDC tablet of the first-line anti-HIV drugs reported. 3DP parameters were optimized and cellulose acetate phthalate (CAP) was added to the HA-PQ10 sludge to enhance the printability (acting as a binder) and gastro-resistance of HA-PQ10. Comparative *in vitro* dissolution studies of the 3DP FDC tablet was undertaken and the *in vivo* performance of the formulation was also investigated in the Large White pig model to establish in-depth quantifiable indicators of drug release and absorption from the gastrointestinal tract (GIT) [16].

2. Materials and methods

2.1. Materials

Brown humic acid sodium salt (HA), hydroxyethylcellulose ethoxylate, quaternized (PQ10 M_w ~ 656.1 g/mol) and cellulose acetate phthalate (CAP M_w = 2534.12 g/mol) were purchased from Sigma-Aldrich® Inc. (St. Louis, Mo, USA). Efavirenz (EFV) (Wenzhou Zhongtai Chemical Co., Ltd, Wenzhou, China), tenofovir disoproxil fumarate (TDF) (Changzhou Yongrui Chemical Research Institute Co., Ltd, Jiangsu, China) and emtricitabine (FTC) (Beijing Zhongshuo Pharmaceutical Technology Development Co., Ltd, Beijing, China) were the model drugs used. UPLC grade water was purified by Milli-Q® gradient water purification system (Millipore SAS, Molsheim, France). Analytical grade methanol and acetone were used as solvents for the sludge synthesis.

2.2. Synthesis and design of the 3DP FDC

Optimization of the tablet shape was conducted by firstly designing different prospective shapes and the configuration yielding the best printability was selected as being ideal for the FDC. SketchUp Pro 2018-64 bit V15.3.331 (Trimble Inc., Sunnyvale, California, United States) was employed to draw the shapes before exporting the .stl files to Magics® software V18.2 (Materialise, Leuven, Belgium) for slicing of the geometries and adjusting the dimensions. Bioplotter RP® V3.0 was used to convert the .stl file to a format compatible with Visual Machine® software on the 3D-Bioplotter®.

3DP of the sludge was undertaken using a 3D-Bioplotter® (EnvisionTEC GmbH, Gladbeck, Germany) equipped with polyethylene cartridges (30 mL) attached to 0.61 mm conical injection nozzles (Nordson EFD, East Providence, Rhode Island, USA). Preparation of the sludge for 3DP involved the hydration of PQ10 (750 mg) with deionized water (3 mL) for 15 min. Methanol (6 mL) was added to EFV/TDF/FTC (1500 mg/750 mg/500 mg) and the mixture was then added to the hydrated PQ10. After adequate mixing, finely ground HA (2250 mg) was added followed by cellulose acetate phthalate (CAP) (1 mL, 12%$^{w}/_{v}$ in acetone). The sludge formulation yielded 5 tablets. The sludge was loaded into the polyethylene cartridge and preliminary designs were produced. Tablet physical attributes such as tablet size, shape and thickness which facilitate fast oesophageal transit time are important to be considered at this stage and would be of paramount importance for further refinement of the 3DP FDC tablet in terms of its Quality Target Product Profile (QTPP) for human trials going forward. Tablet strength was critical to enable the FDC to withstand biomechanical forces in the GIT. QTPP parameters considered in this investigation for designing a prototype system, such as FDC pore structure, bioerosion, swelling and drug release were critical to investigate here in order to manufacture a sustained release FDC that maintained therapeutic drug concentrations for at least 12 h *in vivo*. The Critical Material Attributes (CMAs) of the sludge were viscosity, printability, setting temperature, concentration of CAP and quantity of methanol in order to optimize the nozzle and extrusion-based 3DP process to comply with a 0.61 mm cone injection nozzle. Printing was conducted at an ambient temperature of 25 °C. The Critical 3DP Process Parameters (CPPs) identified from preliminary studies included (1) printing speed, (2) extrusion pressure, and (3) wait-time between layers, which were controlled and preset using built-in algorithms in Visual Machine® software. 3DP was completed using two different formulation approaches. One comprising a sludge consisting of all three FDC drugs (EFV/TDF/FTC) blended together and the second included individual drugs in separate layers of the 3DP tablet. Synthesis of the sludge for the latter approach involved adding methanol to either EFV, TDF, or FTC prior to adding the mixture to PQ10. The 3DP FDCs were left to dry for 12 h at 20 °C. The mean percentage yield of 5 tablets was calculated according to Eq. (1).

$$\%Yield = \frac{Final weight of 3DP FDC tablets}{Initial weight of tablet powder blend} x100 \quad (1)$$

2.3. Determination of 3DP electrostatic stability between formulation components

The test for electrostatic interaction was undertaken to measure the extent of electromagnetic radiation absorption and vibrations resulting from chemical bonds between the drug molecules of EFV/TDF/FTC and HA-PQ10 during the 3DP process. Powdered samples of the formulation components were placed on a diamond crystal of an Attenuated Total Reflectance-Fourier Transform Infrared (ATR-FTIR) spectrophotometer equipped with a single reflection diamond MIRTGS detector (PerkinElmer® Spectrum 100 Series FT-IR Spectrometer PerkinElmerLtd., Beaconsfield, UK). Analysis was conducted over a wavenumber range of 6000–450 cm^{-1}.

2.4. Characterization of surface morphology of the 3DP tablet

The surface morphology of the 3DP tablets was characterized by Scanning Electron Microscopy (SEM) (FEI Nova NanoLab™ 600 DualBeam FIB/SEM, Hillsboro, OR, USA). Thin layers (2 mm) of the 3DP tablets (60° and 90° inner structure patterns) were coated with 10 nm of carbon followed by a 5 nm layer of gold-palladium prior to mounting. The scanning parameters employed were 30 kV at 30 µs.

Imaging was repeated on five different surfaces of the same tablet for consistent and accurate analysis.

2.5. Porositometric analysis of the 3DP FDC

Porositometric analysis, utilizing Brunauer-Emmet-Teller (BET) and Barrett, Joyner and Halenda (BJH) isotherms of nitrogen, was undertaken. The adsorption and desorption profiles were generated to determine the surface area and pore volume of the 3DP FDC. The ASAP 2020 Porositometer with ASAP 202V3.01 software (Micromeritics Instrument Corp., Norcross, GA, USA) was employed for the analysis. Degassing of weighed samples (> 100 mg) placed in isothermal jackets was conducted for 24 h before analysis.

2.6. Mapping of matrix hydration kinetics and gravimetric analysis of the 3DP FDC

The dimensional changes associated with hydration kinetics of the 3DP FDC tablet in simulated intestinal fluid (SIF) were mapped using Magnetic Resonance Imaging (MRI) system (Oxford Instruments Magnetic Resonance, Oxon, UK). MRI has an in-line dissolution flow through cell (USP apparatus 4). SIF was circulated continuously at 4 mL/min and a total of 64 scans were used. Gravimetric analysis was conducted to quantify the amount of moisture absorption of the 3DP FDC in SIF over 24 h. 3DP FDC tablets were accurately weighed then placed into USP 33 type II apparatus (Erweka DT 700, Erweka GmbH, Heusenstamm, Germany) set at 50 rpm and containing SIF at 37 °C. At pre-set intervals the tablets were carefully removed from the apparatus and lightly blotted with paper towel before weighing them to determine any weight changes as time progressed. The study was conducted in triplicate. Eq. (2) was employed to calculate the total equilibrium swelling front at a particular time (t) [17].

$$Watercontent(\%)(t) = \frac{wetmass(t) - drymass(t)}{wetmass(t)} x100 \quad (2)$$

2.7. Prediction of the 3DP FDC tablet matrix strength in bio-relevant media

The 3DP FDC tablet sample was mounted on a BioTester 5000 instrument (CellScale Biomaterials Testing, Waterloo, Ontario) using BioRake tines (1.3 mm). The tablet was firstly hydrated in the respective bio-relevant medium: simulated gastric fluid (SGF, pH = 1.2) or simulated intestinal fluid (SIF, pH = 6.8) for 30 min. The test was undertaken to predict any significant transitions in matrix tensile modulus of the 3DP tablet *in vivo*. Analysis was undertaken on samples submerged in either SGF or SIF at 37 °C. Assessment of the matrix mechanical strength was critical to predict the ability of the 3DP matrix to resist fracture from biomechanical forces likely to be exerted in the GIT. Based on the rectangular prism geometry of the 3DP tablet uniaxial stretching was most ideal using the BioRakes on a Y-axis and 2500 μm apart. A load-cell of 5 N was used and the stretch magnitude utilized to adjust the force to match gastric mechanical forces (1.9 N in the fed state) and intestinal forces of 1.2 N [18]. Image tracking was used to quantify in-plane motions and to directly measure the resultant strains occurring at real-time. Parameters set for the displacement test included a stretch magnitude of 40% for 20 s at 3 cycles. The data collated was utilized to construct stress-strain profiles and the initial linear portion was used to determine the Young's modulus of the 3DP tablet in both SGF and SIF [19].

2.8. Drug-loading and comparative in vitro release testing of the 3DP FDC tablet

The drug-loading capacity in each layer of the 3DP FDC was computed to determine the total number of layers required for dose loading. Drug-loading was determined by firstly printing 2 layers which were used to determine the loading in each tablet layer. The 3DP layers were then immersed in 50 mL SIF (pH 6.8; 37 °C) in an orbital shaker bath for 24 h to ensure complete drug release. This was repeated (N = 6) in order to validate uniform distribution of the three drugs in the sludge during the 3DP process. Drug quantification was determined by UV spectrophotometry (Lambda 25 UV/Vis spectrophotometer, PerkinElmer, MA, USA) at respective wavenumbers for each drug (EFV = 247 nm, TDF = 262 nm and FTC = 281 nm).

Drug release was determined using a USP 33 type II apparatus set at 50 rpm and 37 °C over 24 h. For the first 2 h, drug release testing was undertaken using Fed State Simulated Gastric Fluid (FeSSGF) (500 mL; pH 1.2). This was transitioned to the Fed State Simulated Intestinal Fluid (FeSSIF) (900 mL; pH 6.8) for the remaining 22 h. FeSSIF comprised dissolving NaOH (20.2 g), glacial acetic acid (43.25 g) and NaCl (59.37 g) in deionized water (5 L) and thereafter adjusting the pH to 5.0. Native FeSSIF (500 mL) was used to dissolve sodium taurocholate (59.08 g). Lecithin (59.08 mL) dissolved in methylene chloride (100 mg/mL) was added to the blank FeSSIF. The methylene chloride was eliminated from the emulsion by evaporation and the volume of the media was adjusted to 2 L [20]. Middle stage simulated gastric fluid was prepared by mixing ultra high temperature milk (UHT-milk) (500 mL) with acetate buffer (480 mL). The solution was adjusted to pH 5.0 before adding the acetate buffer to 1 L [21]. Sample aliquots (5 mL) were withdrawn at predetermined times and these were filtered, dried and reconstituted with methanol. Drug release was measured by UV spectrophotometry at the respective wavenumbers for each drug (EFV = 247 nm, TDF = 262 nm and FTC = 281 nm).

2.9. In vivo evaluation of the 3DP tablets in the large white pig model

2.9.1. Experimental design

In vivo animal studies were undertaken following the Principles of Laboratory Animal Care (National Institute of Health, Guide for Care and Use of Laboratory Animals). Ethics clearance was obtained from the Animal Ethics Screening Committee (AESC) at the University of the Witwatersrand, Johannesburg, South Africa (AESC clearance number: 2014/38/C). Jugular vein catheterization was instituted for routine blood sampling (7 French gauge double lumen 35 cm catheter (CS-28702); Arrow Deutschland GmdH, Erding, Germany) performed under aseptic conditions. Pigs were anesthetized using ketamine (11 mg/kg I.M), midazolam (0.3 mg/kg I.M) and topical procaine HCl (0.5%). Vital signs were monitored throughout the procedure. The pigs were allowed 10 days of full recovery before commencement of dosing with the 3DP tablet and comparator formulation [22].

2.9.2. Dosing of the 3DP FDC tablet and comparator formulation

A full standard dose of EFV/TDF/FTC (600 mg/300 mg/200 mg respectively) was administered. Two 3DP FDC tablets (EFV = 300 mg, TDF = 150 mg and FTC = 100 mg in each tablet) was administered for comparison with the market formulation. A baseline blood sample was withdrawn prior to gastric dosing of the pigs in the fasted state via an intragastric tube with 50 mL water. Blood samples were collected at time 0 and 1, 2, 3, 4, 6, 8, 12, 18 and 24 h after dosing in heparinized vacutainers (Improvacuter®, Guangzhou Improve Medical Instruments, Guangzhou, China), centrifuged at 3000 rpm for 15 min before aspirating the plasma supernatant which was then stored in a freezer (−80 °C) for further analysis.

2.9.3. Drug quantification analysis

The collected blood samples were analyzed by Ultra Performance Liquid Chromatography (UPLC) using a Waters® Acquity™ UPLC system (Waters®, Milford, MA, USA) equipped with a binary solvent and sample manager coupled to a photodiode array (PDA) detector. The output signal was monitored by Empower® Pro Software (Waters®, Milford, MA, USA). The instrument was run using an Acquity® UPLC BEH shield RP18 (1.7 μm; 2.1 × 100 mm) column. A modified assay

method for quantifying EFV, TDF and FTC proposed by Induri and co-workers [23] was used. EFV/TDF/FTC were extracted by adding 0.5 mL hexane: ethyl acetate (1:1) to an equal volume of plasma [24]. This was centrifuged for 3 min at 3000 rpm. The top layer was allowed to dry before reconstitution with methanol (0.5 mL) and centrifuged for another 3 min to maximize the extraction of EFV/TDF/FTC.

2.10. Establishment of an in vitro-in vivo correlation (IVIVC) and pharmacokinetic analysis of drug release

To further optimize the FDC, WinNonLin® software (V5.3 with *IVIVC* Toolkit Build 20091211139, Pharsight Software, Statistical Consultants Inc., Apex, NC, USA) was instituted to predict *In Vitro-In Vivo* correlation (IVIVC) of the *in vitro* and *in vivo* release data from all drugs. A Level A *IVIVC* is a mathematical model that establishes a point to point correlation of the *in vitro* dissolution and *in vivo* plasma drug concentration. An *IVIVC* was determined by using the deconvolution and convolution processes. With deconvolution, the Wagner-Nelson [25] method is employed to estimate the observed amount of drug absorbed. The observed fraction of the drug absorbed and that of the drug dissolved is used to develop the appropriate *IVIVC* model. The predicted fraction of drug absorbed is then calculated from the observed fraction dissolved. The convolution method is then implemented to convolve the predicted amount of drug absorbed to the predicted plasma drug concentrations. A Microsoft Excel add-in program written in Visual Basic for Applications (VBA), PKSolver, was employed to conduct pharmacokinetic analysis of the release profiles [26]. Since the system under investigation was an oral tablet, an extravascular compartmental model with Tlag analysis was undertaken. Drug release at specific time points was utilized to calculate the area under the curve *(AUC)*. The calculation took into consideration all the repeat *in vivo* studies conducted. Relative bioavailability (*F*) of 3DP FDC was calculated using Eq. (3) [27].

$$F = \frac{AUC_{0-t(3DPFDC)}}{AUC_{0-t(Atripla^{®})}} \times 100 \quad (3)$$

3. Results and discussion

3.1. Process assessment for the 3DP FDC tablet

3DP was a suitable, flexible technique for exploring the different tablet shapes. From the different geometries explored (Fig. 1), it was concluded that the rectangular prism was optimal for 3DP of the drug-loaded HA-PQ10 sludge. The application of a 3D printer offers flexibility in exploring various intricate tablet shapes and sizes. This is beneficial for allowing the manufacture of varying doses for personalized treatment [1]. The rectangular prism shape yielded a reproducible 3DP device that could be printed to the predetermined tablet full size devoid of any shape deformation.

The tablet composition is represented in Table 1. The calculated mean percentage yield for the 3DP FDC for printing a batch of 5 tablets was 94.35 ± 0.20%. The printing process for the 3DP FDC was efficient with twenty minutes required for printing of a batch of 5 tablets. The layers were printed consecutively for each tablet, with a 30 s wait time elapsing between layers for each tablet while layers for the other tablets were being printed. The efficiency was mainly limited by the drying time of the tablets which was 12 h. Thus a number of tablets could be printed over a 12 h period, which could then all be left overnight to dry. Therefore 15 tablets can be printed in an hour, with up to 180 tablets produced over a 12 h period, which could then be left overnight to dry. This study describes the design of a prototype 3DP FDC system thus further improvements to this process would need to be applied in future studies for scale-up of tablet manufacture.

CAP solution was used as the binder solution in the sludge as well as

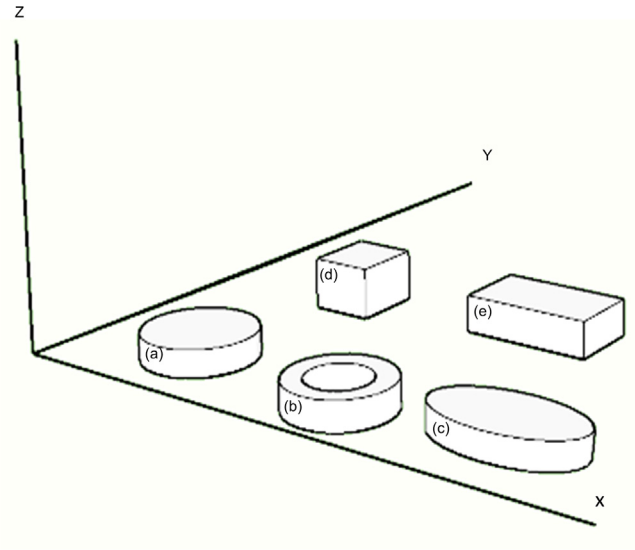

Fig. 1. Tablet shapes designed in Magics® for 3DP of HA-PQ10 as (a) cylindrical, (b) torus, (c) elliptical, (d) cuboid and (e) rectangular prism shapes.

Table 1
Tablet composition and mean % yield.

Tablet composition	Quantity (mg)	% Loading
Efavirenz/Tenofovir/Emtricitabine (EFV/TDF/FTC)	300/150/100	25.5/12.8/8.52
Humic acid (HA)	450	38.3
Polyquaternium10 (PQ10)	150	12.8
Cellulose acetate phthalate (CAP)	24	2.04
Predicted tablet weight	1174	
Tablet mean % yield	94.35 ± 0.204%	

to provide adhesion of the subsequent tablet layers during 3DP. The binder was also expected to improve the hardness of the tablet and subsequently affect the drug release properties [15]. Methanol was responsible for lowering the boiling point of acetone which was employed to dissolve the CAP therefore preventing the 'printing ink'/sludge from drying out while still in the printer cartridge. The inclusion of CAP and methanol thus promoted the synthesis of a pharmaceutically relevant 3D-printable sludge. Fig. 2 depicts digital images of the tablets obtained from 3DP of a sludge containing EFV, TDF and FTC employing the two different designs. Both tablets contained the same drug quantities. 3DP of the sludge containing a blend of EFV/TDF/FTC yielded reproducible tablets. Printing was conducted at an ambient temperature of 25 °C. Preliminary studies revealed that HA-PQ10 was unsuitable for printing at high temperatures therefore the ambient temperature setting was ideal for rendering HA-PQ10 3D-printable. This highlights the instrumental advantages of the 3D-Bioplotter® which operates at a range of low and high temperatures. The optimal 3DP CPPs for the sludge were 1.3 bars extrusion pressure and 37 mm/s printing speed. Pre and post flow delays of 0.05 s were implemented together with a wait time between layers of 30 s. The inner pattern comprised of a 1.2 mm strand distance and to further optimize the formulation, 60° and 90° angles between each layer were explored. As this investigation is still at the preclinical stages, improvements to the evenness and regularity of the 3DP FDC would still need to be undertaken in future studies to render the formulation more suitable for oral administration prior to human studies.

Pharmaceutical materials behave differently during extrusion-based 3DP therefore it was pertinent to determine the optimal tablet shape for the 3DP FDC [2]. 3DP of all three anti-HIV drugs together rather than as separate layers was preferred as 3DP of the TDF-loaded sludge distorted the overall shape and appearance of the tablet. The sludge would need

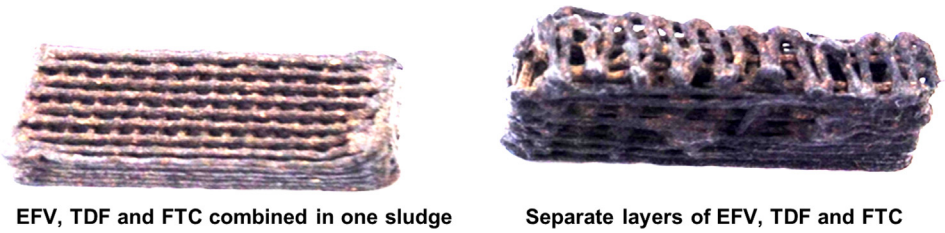

Fig. 2. Digital images of results from two tablet design attempts for 3DP FDC.

to be modified by adding more excipients in order to enhance its 3D-printability. Ultimately, this would increase the size of the 3DP FDC and patient compliance is affected negatively by sizable formulations [28]. Thus, the combined printing of all three anti-HIV drugs method of printing the tablet was selected as it was superior to the alternative approach evaluated as it resulted in the production of reproducible and robust tablets that did not collapse during printing. By 3D-printing, tablet porosity could be altered by varying the alignment of the strands in the tablet, which cannot be implemented with the conventional tableting methods [29].

3.2. Analysis of electrostatic interactions between the HA-PQ10, EFV, TDF and FTC

Due to its predominance, EFV was evident as dominant peaks in the 3DP FDC spectrum while TDF and FTC bands were masked (Fig. 3). The peaks from EFV (exocyclic triple bond = 2278 cm^{-1}, C═O cyclic bond = 1742 cm^{-1} and tertiary amide = 1601 cm^{-1}) expressed in the 3DP FDC were not shifted but the absorbances were diminished due to the presence of the TDF, FTC and HA-PQ10 in the system. The broad band and formation of the two new peaks in the wavenumber region of 3250–3300 cm^{-1} in the 3DP FDC were indicative of drug-polymer hydrogen bond formation as a result of interaction between the NH functional groups of the drugs with the OH functional groups in HA-PQ10 [30]. Furthermore, the broadening of the peak can be attributed to characteristics of the macromolecular HA-PQ10 [7]. This region contains NH bonds from EFV, TDF and FTC as well as OH functional groups from TDF, FTC and HA-PQ10. The small difference in peak absorbance between the 3DP FDC and the drugs and HA-PQ10 indicated that weak drug-polymer hydrogen interactions occurred. This hydrogen bonding between the EFV/TDF/FTC and HA-PQ10 was indicative of possible drug solubility enhancement.

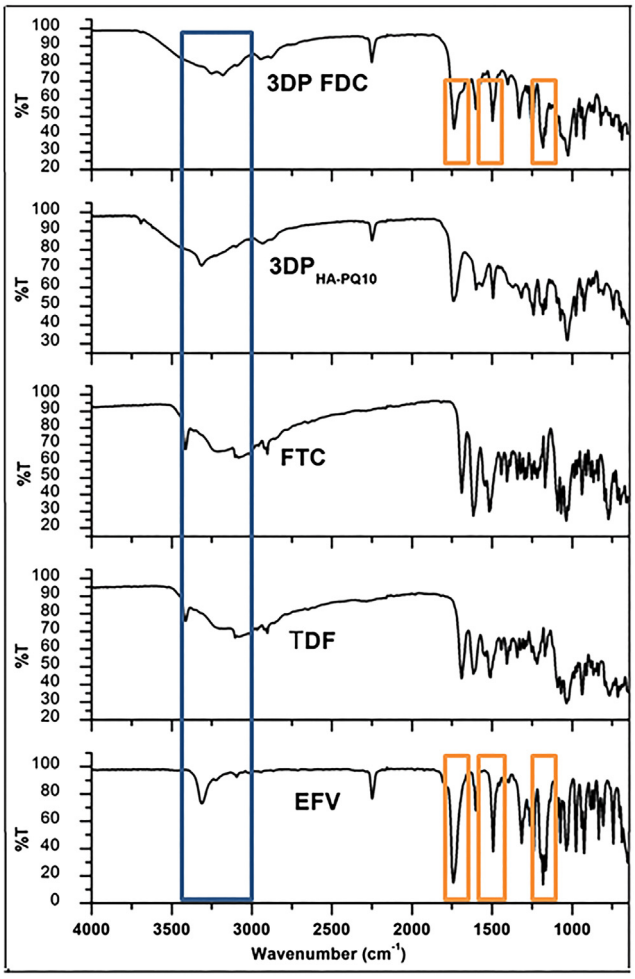

Fig. 3. FTIR spectra of the 3DP FDC in relation to EFV, TDF, FTC and HA-PQ10.

EFV, TDF and FTC were at least partially solubilized due to the addition of methanol during sludge synthesis, in which all 3 drugs are soluble. Our previous investigations of the thermodynamic stability of the drug-loaded HA-PQ10 sludge [7] highlighted the absence of sharp melting endotherms corresponding with that of the crystalline drug in the thermogram, thus signifying the good miscibility of the drug into the polymeric matrix. As discussed therein, the disappearance or shifting of the endotherm of a pure drug is indicative of lack of defined crystalline arrangements. This was attributed to the drug being partially miscible in the matrix and therefore forming a mixed solid dispersion system of amorphous and crystalline drug [7]. This is consistent with the FTIR results reported herein highlighting the occurrence of drug-polymer interactions. Ideal drug-polymer interactions are important for prevention of drug clumping which is responsible for drug polymorphism. The co-existence of the crystalline and amorphous drug forms is beneficial in enhancing drug solubility as well as preventing recrystallization of the bioactives which is common in purely amorphous formulations. HA and PQ-10 being macromolecular in nature, also shield the drug particles from interparticulate interactions responsible for recrystallization [30]. It can thus be deduced that there was a reduction in the crystallinity of the drugs upon dispersion into the HA-PQ10 and the resultant drug-polymer interactions would be expected to elevate the dissolution properties of EFV/TDF/FTC from the 3DP FDC. The presence of hydroxyl groups in the polymers is also indicative of a system that is capable of interacting with gastrointestinal mucosal surfaces through hydrogen bond formation therefore enhancing mucoadhesion, residence time and drug absorption [31].

3.3. Analysis of the surface morphology of the 3DP FDC

SEM imagery provided insight into the exact strand widths and pore sizes created by 3DP with a 0.61 mm injection nozzle creating 60° and 90° inner structure patterns, for establishment of the QTPP of the final FDC tablet. Surface morphology of the tablet at 100x magnification is depicted in Fig. 4a and a closer analysis of the surface at higher magnification, 500x (Fig. 4b), revealed that the 3DP FDC contained a fibrilla structure with evenly dispersed pores. Besides these smaller pores evident on the strands, the inner patterns selected (90° and 60° with 1.2 mm distance) also created pores through gaps between the strands. These patterns were intentionally chosen to increase the ingress of fluid into the system. 3D-printing was thus employed as a versatile technique providing various options for modifying the 3DP FDC tablet geometry,

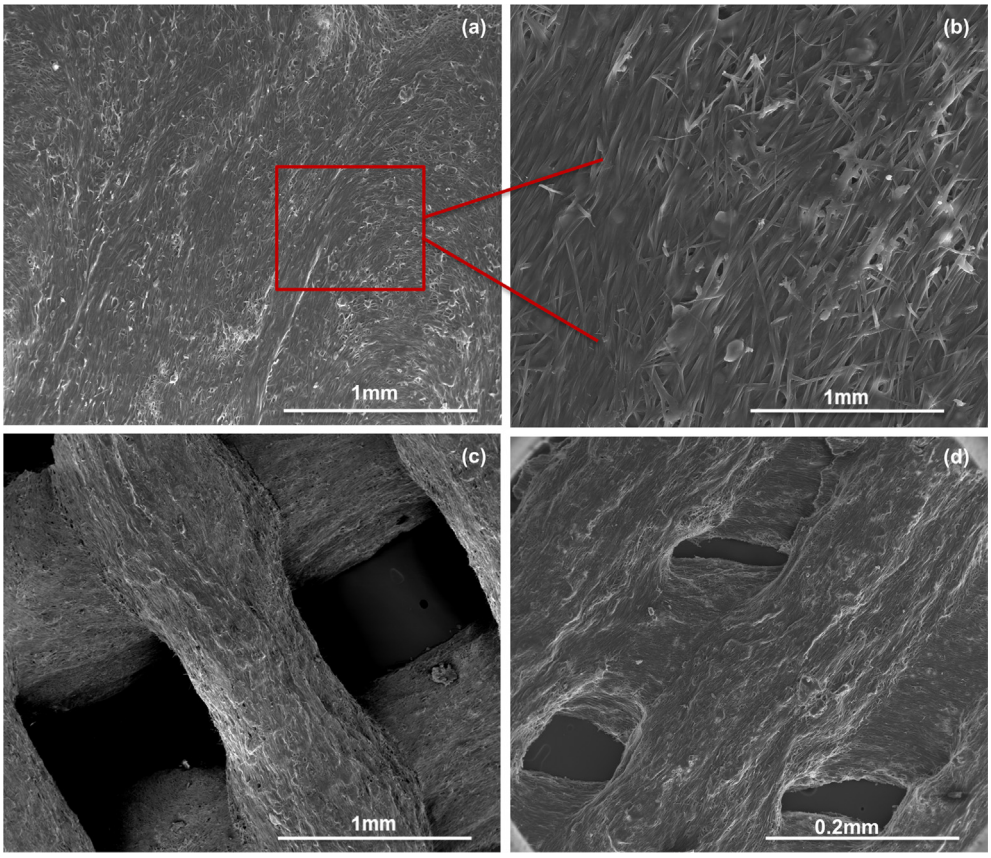

Fig. 4. SEM images of the 3DP FDC at the (a) surface of a strand at 80x magnification, (b) surface of a strand at 500x magnification, (c) alignment of strands at 90° and (d) alignment of strands at 60°.

which is a limitation with conventional tableting techniques [1]. From the images, the final strand thickness and pores created after 3DP could be measured. The tablet with an inner structure pattern of 90° (Fig. 4c) yielded improved strand thickness (0.65 mm) in relation to the injection nozzle size (0.61 mm). The 3DP FDC constructed with the 60° inner pattern yielded thicker strands of 0.88 mm in diameter (Fig. 4d). The thickness of the 3DP FDC tablet with 60° inner structure pattern indicated that smudging occurred during printing [16] therefore the ideal inner structure pattern for the 3DP FDC was 90° between each layer. The fibrilla surface of the 3DP FDC evident in SEM images was expected to facilitate the permeation of the dissolution fluid therefore leading to enhanced tablet hydration.

3.4. Assessment of the porosity of the 3DP FDC tablet

The porositometric test provided a mechanistic understanding of the void spaces in the 3DP FDC tablet. The 3DP FDC exhibited a high surface area and pore volume (Table 2).

Assessment of the isotherm shapes revealed that the porous branches were mostly in a horizontal alignment therefore it was deduced that the 3DP FDC tablet exhibited a type II isotherm characterized by H3 hysteresis loop, indicating the presence of slit-shaped pores in a fibrillar structure, which corresponded with SEM images obtained (Fig. 5 insert). Fig. 5 depicts the isotherms with the quantity of nitrogen adsorbed (cm^3/g STP) plotted against relative pressure (P/P°). 3DP resulted in the formation of interconnected fibrils and pores (red circles) dispersed on the tablet surface. The pores are potential artefacts of solvent evaporation from the sludge, on drying, subsequent to printing.

The overall porosity is expected to determine the extent of interaction of the matrix with the dissolution medium [32]. It is worthwhile to note that correlation of pore surface and dissolution may not always be accurate due to the fact that porosity analysis relies on high pressure nitrogen being forced into the pores of the sample whereas dissolution is dependent on tablet surface properties [33]. The increase in adsorption towards P/P° = 1 was indicative of the presence of pores in 3DP FDC. The tablet had an adsorption average pore width of 2–50 nm therefore it can be concluded that the formulation contained mesopores [34]. Mesoporous surfaces provide a large surface area to volume ratio that enhances wettability of the encapsulated drug. Such surfaces are able to retain high drug doses in the pores for long periods thus they are beneficial in manufacturing controlled release formulations [35].

Table 2
Pore volume and BET surface areas of 3DP FDC.

Parameter		3DP FDC
Surface area	BET surface area	3.0141 ± 0.8324 m^2/g
	Adsorption average pore width (4 V/A by BET)	97.6188 ± 5.6433 Å
Pore volume	BJH adsorption average pore diameter (4 V/A)	125.3430 ± 4.7343 Å
	BJH desorption average pore diameter (4 V/A)	93.2750 ± 1.9150 Å

3.5. MRI mapping and gravimetric analysis of the 3DP FDC tablet

MRI was employed to map solvent mobility in the 3DP FDC tablet. This approach enabled characterization of the hydration dynamics of the 3DP FDC *in situ* for differentiation of and transitions in gelled and non-gelled regions of the tablet. Fig. 6a highlights that the 3DP FDC underwent gradual and homogenous hydration to form a hydrogel structure. The tablet showed a significant increase in size during the study thus confirming its swellability in SIF. Gravimetric analysis

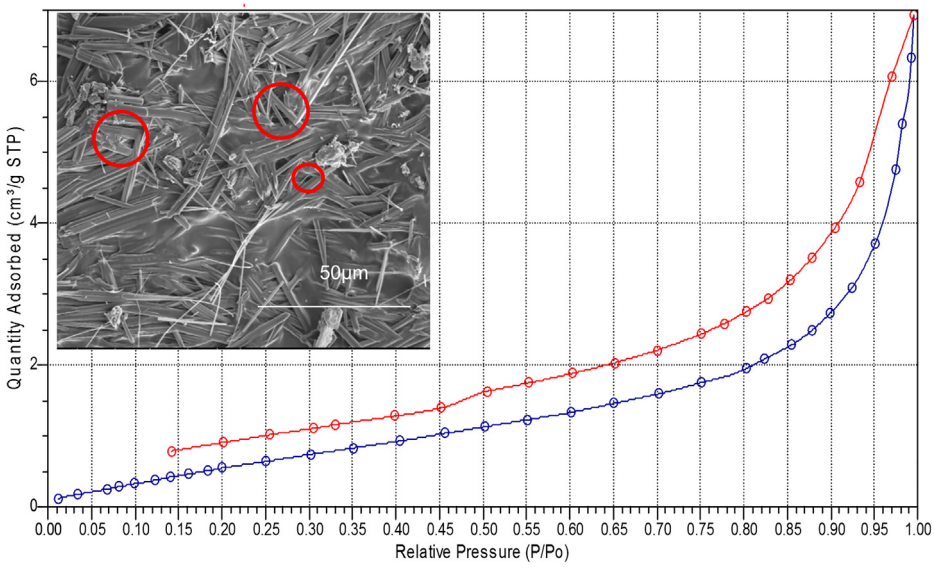

Fig. 5. Isotherm linear plots of the 3DP FDC tablet depicting N_2 adsorption (blue) and desorption (red) with inserts of SEM micrograph of tablet highlighting pores at x2000 magnification. (For interpretation of the references to colour in this figure legend, the reader is referred to the web version of this article.)

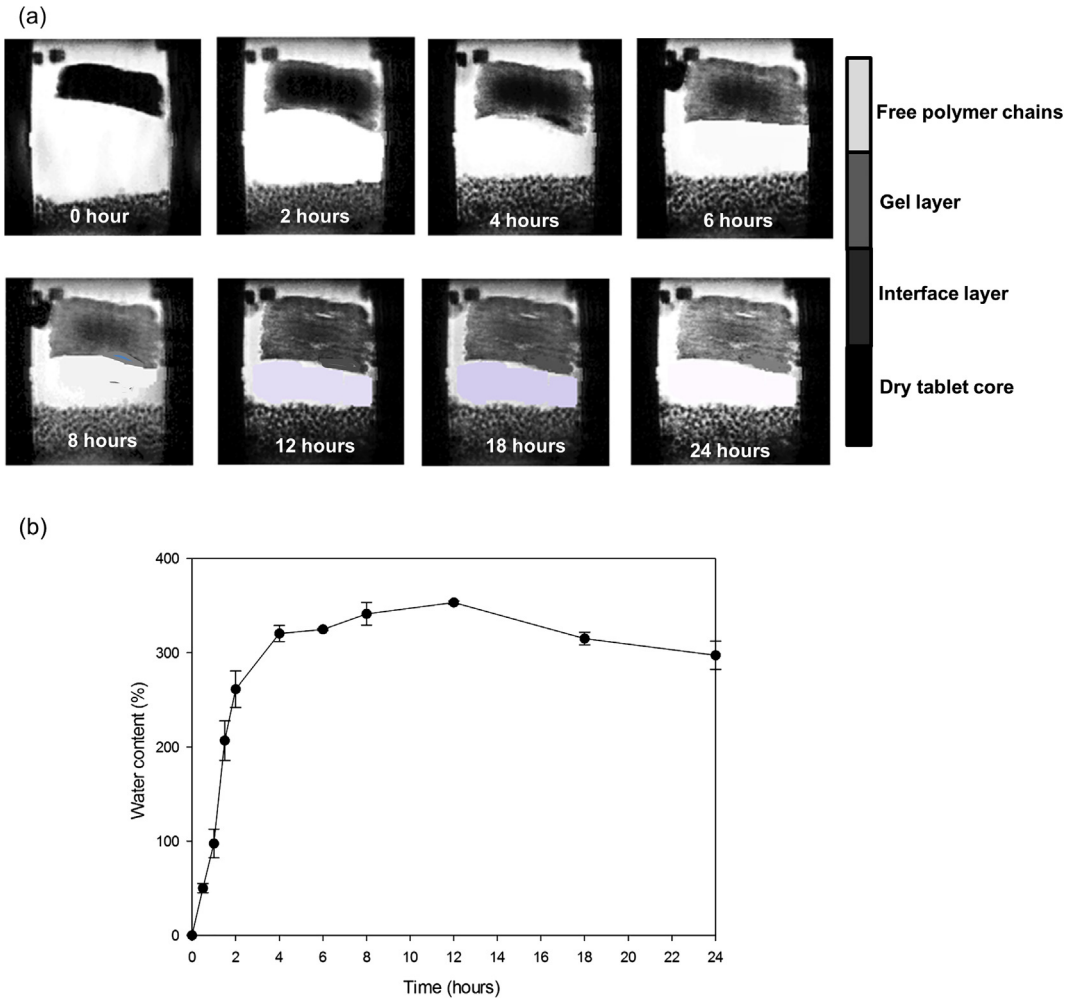

Fig. 6. (a) MRI imaging of the 3DP FDC tablet and (b) 3DP FDC water content during gravimetric analysis.

revealed that SIF permeated into the matrix and reached a maximum hydration of 353.3 ± 8.38% after 12 h at which level it plateaued until the end of the study (Fig. 6b).

Fluid penetration into the matrix resulted in changes in the proton signal of the MRI visualized as an increase in tablet brightness [36]. Observations similar to those made by Kulinowski and co-workers [37] were noted in the MRI images, where 3DP FDC swelled longitudinally and did not disintegrate as the study progressed. The tablet swelled and maintained its dimensional integrity throughout the test period. With the progression of time, it formed a gel layer due to the absorption of SIF and consequent relaxation of the polymer network, thus allowing controlled release of EFV/TDF/FTC. 3DP FDC exhibited 3 phases of hydration kinetics characterized by the dry core, interface layer and gel layer. The dry core is the innermost part of the tablet with limited fluid mobility and this core of the 3DP FDC was no longer visible at 12 h. After 2 h, a surface gel layer could be observed and this continued to swell with hydration expanding inwards towards the core until the 3DP FDC was fully hydrated at 12 h. Thereafter, there were insignificant changes to the tablet size which corresponded with the observed constant drug release rate from that point onwards [17]. The MRI and gravimetric findings indicated that 3DP FDC had good matrix-SIF interaction resulting in swellability of the tablet at a constant rate and therefore drug release was also expected to be constant [38].

3.6. Evaluation of the tensile strength of the 3DP FDC in simulated gastric and intestinal fluid

The image tracking option on the BioTester was implemented to calculate the exact values and spatial variations of the strains that the 3DP FDC was subjected to, based on the motions of the BioRake tines. Fig. 7 shows the digital images of the 3DP FDC exposed to SGF and SIF with inserts of the image tracking as well as the Y-force graph. More strain was exerted towards the periphery of the tablet in both media (red areas). However, higher strain values were demonstrated in SGF with the highest strain of 52.8 recorded, due to gastro-resistance of the FDC tablet. Once submerged in SIF, the tablet hardness decreased as evidenced by the lower strain values (maximum strain 21.3).

Fig. 8 depicts the graphs obtained after 3DP FDC was subjected to forces corresponding to the gastric and intestinal mechanical forces in biorelevant media. The stress-strain graphs (Fig. 8a and c) were used to construct the linear regression graphs (Fig. 8b and d) for further determination of the Young's modulus. Calculation of Young's modulus revealed that the 3DP FDC was more elastic in SGF than SIF with values of 0.117 Pa and 0.113 Pa, respectively.

Tablets should resist mechanical stress in the GIT in order to prevent erratic tablet erosion. Formulation of tablets with good resistance maximizes the chance of more accurate *in vitro-in vivo* correlation profiles. Solid dosage forms are liable to losing their tensile strengths when hydrated [18]. The 3DP FDC exhibited a higher mechanical strength in SGF where it did not absorb the dissolution fluid readily. This characteristic was expected since CAP is insoluble in SGF [39]. CAP became solvated in SIF therefore elevating matrix-fluid interaction. The 3DP FDC was more elastic in SIF as the pH was more favourable for fluid ingress into the tablet. This attribute had an effect on the solubility of drugs as adequate fluid sorption into the system increases drug wettability [40]. Despite the differences in behavior of the 3DP FDC in SGF and SIF, the tablet maintained its tensile strength modulus and did not fracture in either SGF or SIF during movement of the BioRakes. The calculated values for the Young's Modulus suggested that the overall nature of the tablet was amorphous, as crystalline materials would be expected to demonstrate higher moduli [41].

3.7. Analysis of drug loading and the in vitro drug release profiles of the 3DP FDC and atripla®

The rectangular prism tablet dimensions were adjusted to accommodate the drug loading and the final dimensions were 2.3 cm × 0.8 cm × 1.2 cm, which was ascertained to be the optimal size for this formulation from preliminary investigations for incorporating the required dosage of all drugs while preventing collapse of the tablet layers. A total of 24 layers per tablet were printed and drug loading in each layer was determined to be 12.5 ± 0.07 mg/6.3 ± 0.41 mg/4 ± 0.04 mg of EFV/TDF/FTC, respectively. The FDA recommends that the largest dimension of a tablet should not exceed 2.2 cm [42], thus further slight refinement in size is required to promote ease of swallowing prior to progression to human studies. The rate of release was related to the hydration of the tablet with controlled release of all drugs over the first 12 h from the 3DP FDC compared to Atripla®, specifically for TDF and FTC (Fig. 9). EFV demonstrated extended controlled release from the 3DP FDC over the 24 h period of investigation. Release in SGF (first 2 h) was limited by the presence of CAP in the system which is insoluble in acidic media. CAP served as an initial diffusion barrier thus limiting water access to the matrix in SGF. The small amount of drug that dissolved was attributed to the exposed surface drug. Drug release from 3D-printed formulations is not expected to occur by disintegration as is the case in tablets manufactured via powder compaction due to the absence of strain recovery in the tablet. Application of 3D-printing vs. conventional tabletting techniques ultimately yields a notably different configuration and surface areas which impacts on the drug release properties of 3DP systems [9,15].

Swelling of the 3DP FDC to form a hydrogel structure facilitated drug release by allowing the SIF to gain access to the entrapped drug [43]. The observed swelling of 3DP FDC occurred due to the decrease in charge density with subsequent drug dissolution. However, in this

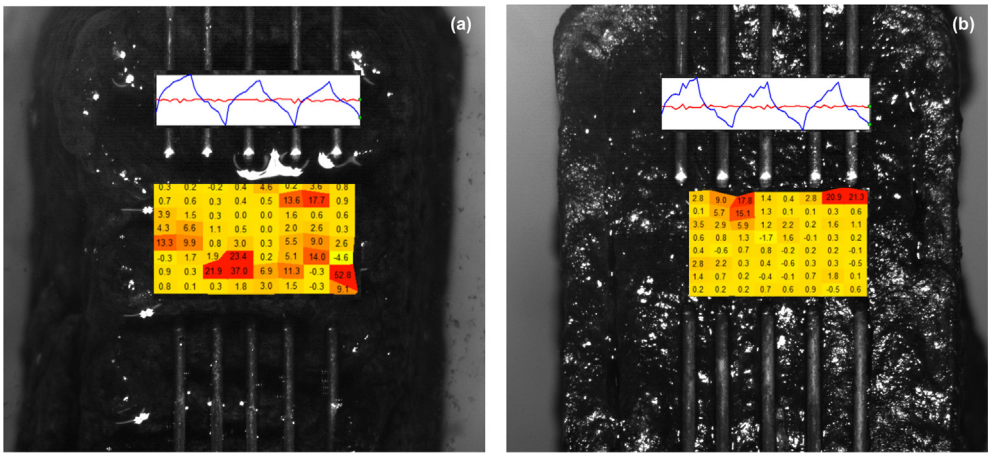

Fig. 7. Digital Biotester images of 3DP FDC and corresponding strains and Y-force graphs in (a) SGF and (b) SIF.

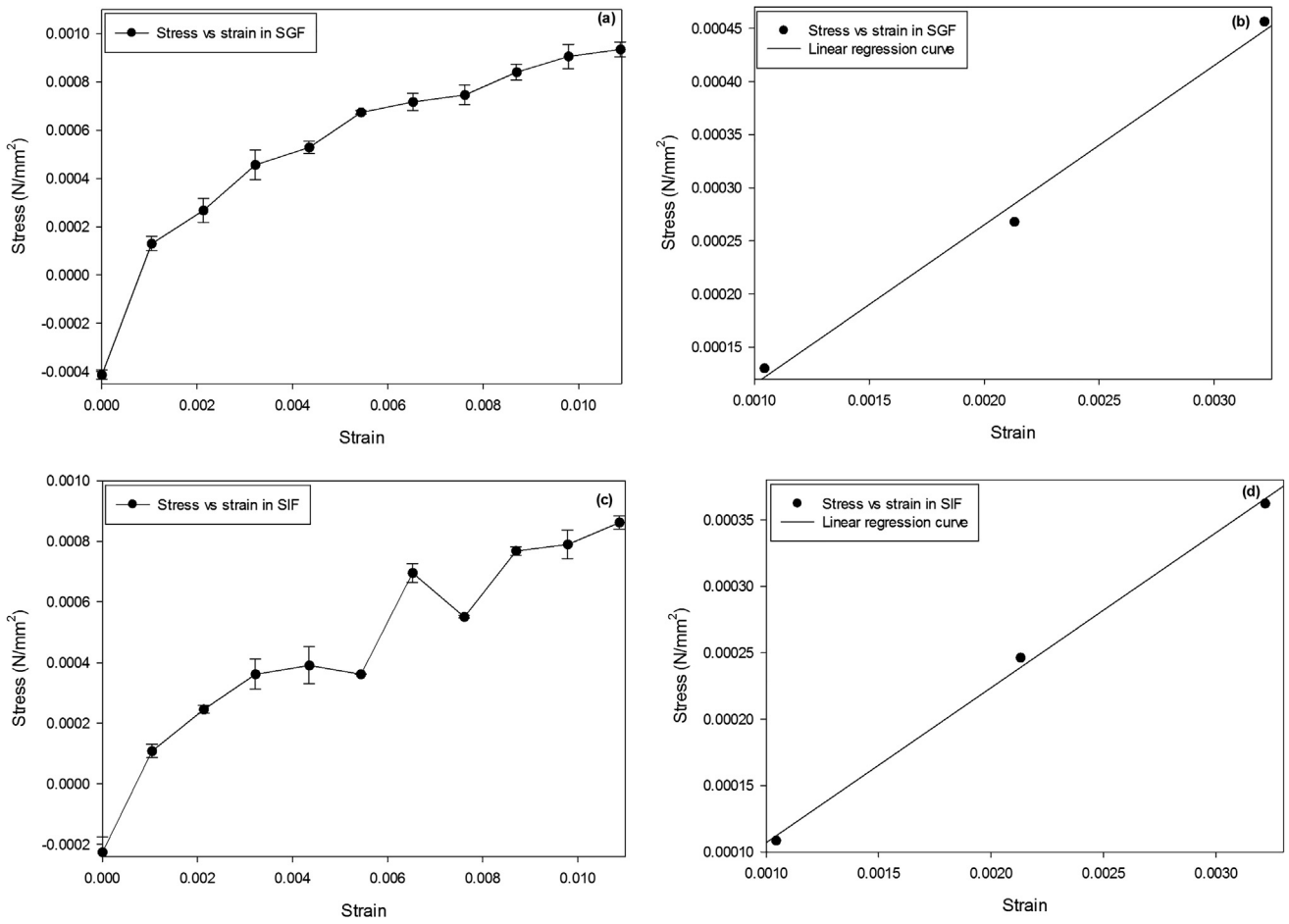

Fig. 8. Stress-strain graphs of (a) 3DP FDC submerged in SGF, (b) initial linear curve in SGF, (C) 3DP FDC submerged in SIF and (d) initial liner curve in SIF.

study, the rate of drug release was retarded by the formation of a strong gel due to the macromolecular nature of HA-PQ10 [19,44]. The sustained release exhibited from the 3DP FDC was attributed to the complexation in HA-PQ10 which limited movement of the entrapped drugs into the dissolution medium.

3.8. *In vivo drug release profiles of 3DP FDC in comparison to atripla®*

EFV, TDF and FTC were eluted from the UPLC column within a run time of 3 min and retention times were 0.98 min (FTC), 1.51 min (TDF) and 1.71 min (EFV). The plasma drug release profiles for 3DP FDC and Atripla® are depicted in Fig. 10. The *in vivo* release profiles for the 3DP FDC indicated that drug release mostly occurred in the intestinal region for all drugs regardless of their BCS class. The simultaneous controlled drug release was also ascribed to the complexation of a hydrophilic (PQ10) and amphiphilic polymer (HA) forming the HA-PQ10 matrix. HA served the purpose of entrapping the lipophilic drugs in the hydrophobic core as previously reported by our group [6,7]. Furthermore, Punčochová and co-workers [45] reported that amphiphilic polymers prevent drug recrystallization during dissolution and this creates a microenvironment of saturated and solubilized drug particles. EFV and TDF were trapped in the hydrophobic core of amphiphilic HA due to their lipophilicity and this enhanced their dissolution and absorption across the intestinal membrane. Absorption of EFV and TDF was further improved as the pigs were fed and this led to a higher drug absorption compared to that noted in the dissolution study. HA-PQ10 proposedly altered the tight junction proteins of the intestinal epithelia thus enhancing paracellular transport of EFV/TDF/FTC into the systemic circulation [46]. Absorption-enhancing polymers usually present with potential toxicity *in vivo* [47]; however, previous studies undertaken by our group [6,7] corroborated with the *in vivo* study that the HA-PQ10 was biocompatible. TDF and FTC are subject to intracellular phosphorylation which largely determines the absorption of the drugs [15]. The phosphorylation which occurred *in vivo* is the reason both drugs had markedly higher concentrations than the maximum concentration reached *in vitro*. The 3DP FDC is proposed to have an increased GI retention time from the known 6–8 h attributed to the swellability of the 3DP FDC, with the water content of the tablet increasing to over 300% by 4 h. The tablet size has been reported to have an impact on the retention time with expandable oral drug delivery systems (such as the reported 3DP tablet that attains a notably larger size due to swelling) remaining in the GIT for longer periods [2]. Additionally, the blood samples were collected from pigs that were in the fed state and this is expected to delay the GI motility of the dosage form.

3.9. *Assessment of in vitro-in vivo correlation and pharmacokinetic analysis of EFV/TDF/FTC in 3DP FDC*

Level A assessment of the *in vitro* and *in vivo* results led to the development of a correlation between the two which gave insight on the predictive accuracy of the *in vitro* analysis employed. Deconvolution was achieved by using the Wagner Nelson method to calculate the concentration of the drugs absorbed using the linear trapezoidal rule. Although *in vitro* drug release studies were conducted in biologically relevant media, high sheer rates in physiological conditions are responsible for more rapid tablet disintegration than in *in vitro* conditions [48]. These conditions cannot be accurately simulated during dissolution studies with a paddle apparatus. EFV and TDF reached maximum

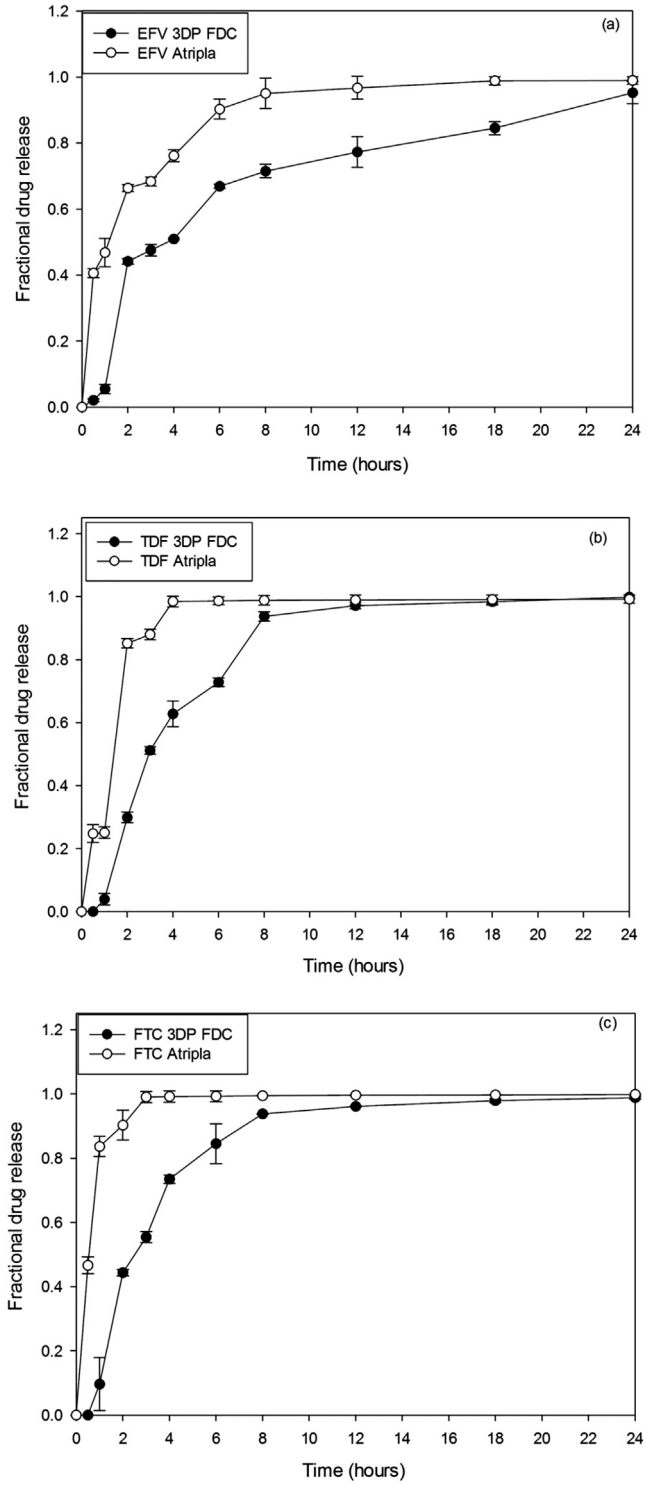

Fig. 9. Drug release profiles of (a) EFV, (b) TDF and (c) FTC in 3DP FDC compared to Atripla®.

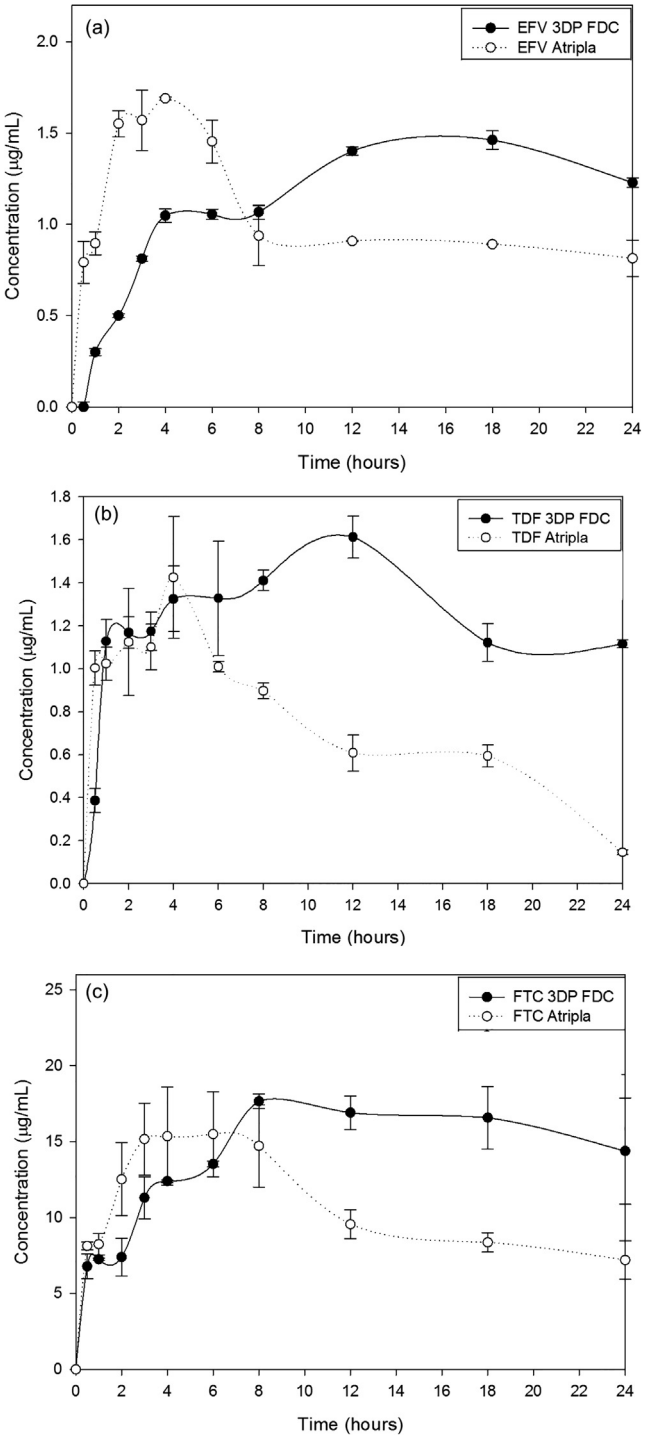

Fig. 10. *In vivo* plasma drug concentrations for (a) EFV, (b) TDF and (c) FTC.

concentrations later than was predicted from the *in vitro* studies. Both these active pharmaceutical ingredients (APIs) exhibit bioavailability limitations with EFV being poorly soluble (lipophilic) and TDF containing a diester derivative responsible for its lipophilicity in an effort to enhance its systemic exposure. After convolution, the correlation of *in vitro* and *in vivo* EFV release and absorption was best described using the correlation plot (fraction absorbed vs. fraction dissolved) which yielded a 85.17% level of accuracy of correlation of the fraction of drug absorbed in relation to that released. TDF and FTC release and absorption were best described by the Levy plot (time to percentage absorbed vs. time to percentage dissolved) with 87.32% and 96.96% accuracies, respectively. The *IVIVC* results suggested that the *in vitro* test conducted resulted in a slower initial drug release but that the maximum concentration was reached more rapidly.

Pharmacokinetic analysis revealed that the maximum plasma drug concentration (C_{max}) for all drugs was achieved after 6 h for the 3DP FDC compared to Atripla® therefore the test formulation provided controlled release of EFV/TDF/FTC (Table 3). The half-lives ($t_{½}$) for TDF and FTC have been recorded as approximately 9 h and 5 h, respectively [12]. Attainment of sustained therapeutic levels of these

Table 3
Pharmacokinetic parameters calculated via PKSolver for the 3DP FDC and Atripla®.

Drug	Parameter	Formulation	
		3DP FDC	Atripla®
Efavirenz			
	T_{max} (h)	14.85	3.16
	C_{max} (μg/mL)	1.36	1.51
	$AUC_{0\text{-}t}$ (μg/mL*h)	27.79	25.28
	$AUC_{0\text{-}inf}$ (μg/mL*h)	167.07	39.97
	F (%)	109.93	
Tenofovir			
	T_{max} (h)	4.88	3.68
	C_{max} (μg/mL)	1.38	1.38
	$AUC_{0\text{-}t}$ (μg/mL*h)	29.89	13.66
	$AUC_{0\text{-}inf}$ (μg/mL*h)	162.51	13.81
	F (%)	218.83	
Emtricitabine			
	T_{max} (h)	11.01	4.04
	C_{max} (μg/mL)	16.45	15.43
	$AUC_{0\text{-}t}$ (μg/mL*h)	348.66	259.27
	$AUC_{0\text{-}inf}$ (μg/mL*h)	2166.43	395.65
	F (%)	134.47	

drugs for an extended period would thus be useful for enabling once daily dosing. The drug release concentrations from a 24 h study were found to be inadequate for measuring the $t_{½}$ of EFV. The $t_{½}$ has however, been estimated to be 40–55 h [12]. The C_{max} recorded for EFV release from Atripla® exceeded the C_{max} predicted (Table 3) and observed (Fig. 10) for the same drug from 3DP FDC. However, slow release of EFV is beneficial given that the drug has a narrow therapeutic index and is associated with neuropsychiatric effects when plasma drug concentrations are increased. Further, as discussed, EFV suffers from bioavailability limitations based on its poor solubility. The therapeutic interval of EFV has been set at 1–4 μg/mL [49] and the EFV plasma levels from 3DP FDC were sustained within this window from 4 to 24 h, whereas EFV levels from Atripla® fall below the minimum effective level from ~8 h. The predicted (Table 3) and observed (Fig. 10) TDF and FTC C_{max} values from the 3DP FDC were the same or slightly higher than for the corresponding drug levels from Atripla®, respectively, and these levels were also sustained for the 24 h period of investigation. Notably, $AUC_{0\text{-}\infty}$ values were consistently higher for all bioactives for the 3DP FDC compared to Atripla®. Area under the curve ($AUC_{0\text{-}\infty}$) is a reflection of the extent of *in vivo* drug absorption and it is directly proportional to the T_{max} of the drug [27]. $AUC_{0\text{-}t}$ was utilized to calculate *F* for EFV/TDF/FTC from the 3DP FDC and all the *F* values were above 100% (Table 2) indicating an enhanced relative bioavailability of all three anti-HIV drugs from the 3DP FDC compared to Atripla®.

4. Conclusions

Extrusion-based 3DP is a versatile tool that allows the control of object geometries to customize them for the 'printing ink' as well as for the intended purpose of the 3DP object. A novel bioink comprising cellulose acetate phthalate and methanol, humic acid-polyquaternium 10 complex was formulated that was 3D-printable into a multidrug solid dosage form at ambient conditions. Optimization of the 3DP FDC design involved consideration of the tablet geometry and exploration of different inner structure patterns. The rectangular prism shape with strands printed at 90° angle provided desired results for 3D-printing the FDC. *In vivo* analysis of the anti-HIV drugs loaded in the 3DP FDC confirmed the successful controlled and intestinal targeted release mechanism from the delivery system. The pH-modulated system allowed for the simultaneous delivery and release of three drugs belonging to different BCS classes. The maximum drug concentrations absorbed were superior for tenofovir and emtricitabine compared to the same drugs from the conventional tablet. Though efavirenz plasma concentration from the 3DP FDC was slightly lower than the concentration of the same drug from Atripla®, sustained release within the therapeutic index (without toxic levels) was achieved throughout the 24 h test period. Further development of the 3DP FDC would involve in depth studies comparing the effect of the EFV, TDF and FTC concentrations from the 3DP tablet on liver enzymes compared to the market comparator to identify any advantages conferred by the controlled release system. Additionally, based on the findings of this study, it will be pertinent to determine any possible dose reduction that could be afforded by the controlled release 3DP system which would consequently minimize the unpleasant side effects commonly associated with the use of these drugs. Furthermore, as highlighted, refinement in terms of the QTPP and scale-up of the 3DP FDC tablet is required to promote ease of swallowing prior to progression to human studies.

Acknowledgements

This work was funded by the National Research Foundation (NRF) of South Africa.

Conflict of interest

The authors confirm that there are no conflicts of interest.

References

[1] A. Goyanes, A.B. Buanz, A.W. Basit, S. Gaisford, Fused-filament 3D printing (3DP) for fabrication of tablets, Int. J. Pharm. 476 (1) (2014) 88–92.
[2] A. Goyanes, P.R. Martinez, A. Buanz, A.W. Basit, S. Gaisford, Effect of geometry on drug release from 3D printed tablets, Int. J. Pharm. 494 (2) (2015) 657–663.
[3] L. Moroni, R. Schotel, J. Sohier, J.R. de Wijn, C.A. van Blitterswijk, Polymer hollow fiber three-dimensional matrices with controllable cavity and shell thickness, Biomaterials 27 (35) (2006) 5918–5926.
[4] T.C. Okwuosa, D. Stefaniak, B. Arafat, A. Isreb, K.W. Wan, M.A. Alhnan, A lower temperature FDM 3D Printing for the manufacture of patient-specific immediate release tablets, Pharm. Res. 33 (11) (2016) 2704–2712.
[5] M. Siyawamwaya, Y.E. Choonara, D. Bijukumar, P. Kumar, L.C. du Toit, V. Pillay, A review: overview of novel polyelectrolyte complexes as prospective drug bioavailability enhancers, Int. J. Polym. Mater. 64 (18) (2015) 955–968.
[6] M. Siyawamwaya, Y.E. Choonara, P. Kumar, P.P. Kondiah, L.C. du Toit, V. Pillay, A humic acid-polyquaternium-10 stoichiometric self-assembled fibrilla polyelectrolyte complex: Effect of pH on synthesis, characterization, and drug release, Int. J. Polym. Mater. 65 (11) (2016) 550–560.
[7] M. Siyawamwaya, Y.E. Choonara, P. Kumar, P.P. Kondiah, L.C. du Toit, V. Pillay, Synthesis, comparison, and optimization of a humic acid-quat10 polyelectrolyte complex by complexation-precipitation versus extrusion-spheronization, AAPS PharmSciTech. 18 (8) (2017) 3116–3128.
[8] W.E. Katstra, R.D. Palazzolo, C.W. Rowe, B. Giritlioglu, P. Teung, M.J. Cima, Oral dosage forms fabricated by three dimensional printing™, J. Control. Release. 66 (1) (2000) 1–9.
[9] D. Markl, J.A. Zeitler, C. Rasch, M.H. Michaelsen, A. Müllertz, J. Rantanen, T. Rades, J. Bøtker, Analysis of 3D prints by x-ray computed microtomography and terahertz pulsed imaging, Pharm Res. 34 (5) (2017) 1037–1052.
[10] N. Scoutaris, S. Ross, D. Douroumis, Current trends on medical and pharmaceutical applications of inkjet printing technology, Pharm. Res. 33 (8) (2016) 1799–1816.
[11] J. Norman, R.D. Madurawe, C.M. Moore, M.A. Khan, A. Khairuzzaman, A new chapter in pharmaceutical manufacturing: 3D-printed drug products, Adv. Drug Deliv. Rev. 108 (2017) 39–50.
[12] M. Lamorde, P. Byakika-Kibwika, W.S. Tamale, F. Kiweewa, M. Ryan, A. Amara, J. Tjia, D. Back, S. Khoo, M. Boffito, C. Kityo, Effect of food on the steady-state pharmacokinetics of tenofovir and emtricitabine plus efavirenz in Ugandan adults, AIDS Res. Treat. (2012), http://dx.doi.org/10.1155/2012/105980.
[13] F. Ravenelle, R.H. Marchessault, A. Legare, M.D. Buschmann, Mechanical properties and structure of swollen crosslinked high amylose starch tablets, Carbohydr. Polym. 47 (3) (2002) 259–266.
[14] C.C. Sun, Microstructure of tablet-pharmaceutical significance, assessment, and engineering, Pharm. Res. 34 (5) (2017) 918–928.
[15] S.A. Khaled, J.C. Burley, M.R. Alexander, C.J. Roberts, Desktop 3D printing of controlled release pharmaceutical bilayer tablets, Int. J. Pharm. 461 (1) (2014) 105–111.
[16] M. Jensen-Waern, M. Andersson, R. Kruse, B. Nilsson, R. Larsson, O. Korsgren, B. Essén-Gustavsson, Effects of streptozotocin-induced diabetes in domestic pigs with focus on the amino acid metabolism, Lab. Anim. 43 (3) (2009) 249–254.
[17] X. Yin, H. Li, Z. Guo, L. Wu, F. Chen, M. de Matas, Q. Shao, T. Xiao, P. York, Y. He, J. Zhang, Quantification of swelling and erosion in the controlled release of a poorly water-soluble drug using synchrotron x-ray computed microtomography, AAPS J.

15 (4) (2013) 1025–1034.
[18] R. Ali, A. Dashevsky, R. Bodmeier, Poly vinyl acetate and ammonio methacrylate copolymer as unconventional polymer blends increase the mechanical robustness of HPMC matrix tablets, Int. J. Pharm. 516 (1) (2017) 3–8.
[19] P. Sriamornsak, N. Thirawong, Y. Weerapol, J. Nunthanid, S. Sungthongjeen, Swelling and erosion of pectin matrix tablets and their impact on drug release behavior, Eur. J. Pharm Biopharm. 67 (1) (2007) 211–219.
[20] S. Viral, P. Dhiren, S. Mane, U. Umesh, Solubility and dissolution rate enhancement of licofelone by using modified guar gum, Int. J. PharmTechRes. 2 (3) (2010) 1847–1854.
[21] E. Jantratid, N. Janssen, C. Reppas, J.B. Dressman, Dissolution media simulating conditions in the proximal human gastrointestinal tract: an update, Pharm. Res. 25 (7) (2008) 1663.
[22] H. Jørgensen, A. Serena, P.K. Theil, R.M. Engberg, Surgical techniques for quantitative nutrient digestion and absorption studies in the pig, Livest. Sci. 133 (1) (2010) 57–60.
[23] M. Induri, B.R. Mantripragada, R.P. Yejella, Development and validation of UPLC method for simultaneous estimation of efavirenz and lamivudine in pharmaceutical formulations, J. App. Pharm. Sci. 6 (3) (2016) 29–33.
[24] L.B. Avery, T.L. Parsons, D.J. Meyers, W.C. Hubbard, A highly sensitive ultra performance liquid chromatography–tandem mass spectrometric (UPLC–MS/MS) technique for quantitation of protein free and bound efavirenz (EFV) in human seminal and blood plasma, J. Chromatogr. B 878 (31) (2010) 3217–3224.
[25] Y. Wang, J. Nedelman, Bias in the Wagner-Nelson estimate of the fraction of drug absorbed, Pharm. Res. 19 (4) (2002) 470–476.
[26] Y. Zhang, M. Huo, J. Zhou, S. Xie, PKSolver: An add-in program for pharmacokinetic and pharmacodynamic data analysis in Microsoft Excel, Comput Methods Programs Biomed. 99 (3) (2010) 306–314.
[27] L. Wang, R. Feng, J. Gao, Y. Xi, G. Huang, Generic sustained release tablets of trimetazidine hydrochloride: preparation and in vitro–in vivo correlation studies, Asian J. Pharm. Sci. 11 (3) (2016) 417–426.
[28] B. Jimmy, J. Jose, Patient medication adherence: measures in daily practice, Oman Med. J. 26 (3) (2011) 155.
[29] D. Klose, F. Siepmann, K. Elkharraz, S. Krenzlin, J. Siepmann, How porosity and size affect the drug release mechanisms from PLGA-based microparticles, Int. J. Pharm. 314 (2) (2006) 198–206.
[30] S.K. Sathigari, V.K. Radhakrishnan, V.A. Davis, D.L. Parsons, R.J. Babu, Amorphous-state characterization of efavirenz—polymer hot-melt extrusion systems for dissolution enhancement, J. Pharm. Sci. 101 (9) (2012) 3456–3464.
[31] J. Boateng, J. Mani, F. Kianfar, Improving drug loading of mucosal solvent cast films using a combination of hydrophilic polymers with amoxicillin and paracetamol as model drugs, BioMed Res. Int. (2013), http://dx.doi.org/10.1155/2013/198137.
[32] G. Gonzalez, A. Sagarzazu, T. Zoltan, Infuence of microstructure in drug release behavior of silica nanocapsules, J. Drug Deliv. (2013), http://dx.doi.org/10.1155/2013/803585.
[33] M. Riippi, J. Yliruusi, T. Niskanen, J. Kiesvaara, Dependence between dissolution rate and porosity of compressed erythromycin acistrate tablets, Eur. J. Pharm. Biopharm. 46 (2) (1998) 169–175.
[34] K.S. Sing, Reporting physisorption data for gas/solid systems with special reference to the determination of surface area and porosity (Recommendations 1984), Pure Appl. Chem. 54 (1982) 2201, http://dx.doi.org/10.1351/pac198254112201.
[35] H.A. Santos, J. Salonen, L.M. Bimbo, V.P. Lehto, L. Peltonen, J. Hirvonen, Mesoporous materials as controlled drug delivery formulations, J. Drug Deliv. Sci. Technol. 21 (2) (2011) 139–155.
[36] M. Shapiro, M.A. Jarema, S. Gravina, Magnetic resonance imaging of an oral gastrointestinal-therapeutic-system (GITS) tablet, J. Control. Release. 38 (2–3) (1996) 123–127.
[37] P. Kulinowski, P. Dorożyński, A. Młynarczyk, W.P. Węglarz, Magnetic resonance imaging and image analysis for assessment of HPMC matrix tablets structural evolution in USP apparatus 4, Pharm. Res. 28 (5) (2011) 1065–1073.
[38] R.D. Sinha, B.D. Rohera, Comparative evaluation of rate of hydration and matrix erosion of HEC and HPC and study of drug release from their matrices, Eur. J. Pharm. Sci. 16 (3) (2002) 193–199.
[39] S.R. Béchard, L. Levy, S.D. Clas, Thermal, mechanical and functional properties of cellulose acetate phthalate (CAP) coatings obtained from neutralized aqueous solutions, Int. J. Pharm. 114 (2) (1995) 205–213.
[40] I. Sideridou, V. Tserki, G. Papanastasiou, Study of water sorption, solubility and modulus of elasticity of light-cured dimethacrylate-based dental resins, Biomaterials 24 (4) (2003) 655–665.
[41] S.J. Eichhorn, R.J. Young, The Young's modulus of a microcrystalline cellulose, Cellulose 8 (3) (2001) 197–207.
[42] K.R. Karst, A hard pill to swallow? in transit for a couple of years, FDA finally coughs up draft guidance on physical attributes of generic tablets and capsules. December 15, 2013. http://www.fdalawblog.net/2013/12/a-hard-pill-to-swallow-in-transit-for-a-couple-of-years-fda-finally-coughs-up-draft-guidance-on-phys/. (Accessed 28/02/2018).
[43] S.L. Harilall, Y.E. Choonara, G. Modi, L.K. Tomar, C. Tyagi, P. Kumar, L.C. du Toit, S.E. Iyuke, M.P. Danckwerts, V. Pillay, Design and pharmaceutical evaluation of a nano-enabled crosslinked multipolymeric scaffold for prolonged intracranial release of zidovudine, J. Pharm. Sci. 16 (3) (2013) 470–485.
[44] M. Buriuli, D. Verma, Polyelectrolyte complexes (PECs) for biomedical applications, Adv. Biomater. Biomed. Appl. Singapore: Springer; Adv. Struct. Mater. 66 (2017) 45–93, http://dx.doi.org/10.1007/978-981-10-3328-5_2.
[45] K. Punčochová, A.V. Ewing, M. Gajdošová, T. Pekárek, J. Beránek, S.G. Kazarian, F. Štěpánek, The combined use of imaging approaches to assess drug release from multicomponent solid dispersions, Pharm. Res. 34 (5) (2017) 990–1001.
[46] A. Parr, I.J. Hidalgo, C. Bode, W. Brown, M. Yazdanian, M.A. Gonzalez, K. Sagawa, K. Miller, W. Jiang, E.S. Stippler, The effect of excipients on the permeability of BCS Class III compounds and implications for biowaivers, Pharm. Res. 33 (1) (2016) 167–176.
[47] S. Shubber, D. Vllasaliu, C. Rauch, F. Jordan, L. Illum, S. Stolnik, Mechanism of mucosal permeability enhancement of CriticalSorb®(Solutol® HS15) investigated in vitro in cell cultures, Pharm. Res. 32 (2) (2015) 516–527.
[48] D.M. Mudie, G.L. Amidon, G.E. Amidon, Physiological parameters for oral delivery and in vitro testing, Mol. Pharm. 7 (5) (2010) 1388–1405.
[49] L. Ståhle, L. Moberg, J.O. Svensson, A. Sönnerborg, Efavirenz plasma concentrations in HIV-infected patients: inter-and intraindividual variability and clinical effects, Ther. Drug Monit. 26 (3) (2004) 267–270.